Oscillating electric-field effects on adsorbed-water at rutile- and anatase-TiO_2 surfaces

Zdenek Futera, and Niall J. English

Citation: The Journal of Chemical Physics **145**, 204706 (2016);
View online: https://doi.org/10.1063/1.4967520
View Table of Contents: http://aip.scitation.org/toc/jcp/145/20
Published by the American Institute of Physics

Oscillating electric-field effects on adsorbed-water at rutile- and anatase-TiO_2 surfaces

Zdenek Futera[a] and Niall J. English[a]
School of Chemical and Bioprocess Engineering, University College Dublin, Belfield, Dublin 4, Ireland

(Received 28 September 2016; accepted 26 October 2016; published online 29 November 2016)

We have performed non-equilibrium molecular dynamics simulations of various TiO_2/water interfaces at ambient temperature in presence of oscillating electric fields in frequency range 20–100 GHz and RMS intensities 0.05–0.25 V/Å. Although the externally applied fields are by one order of magnitude lower than the intrinsic electric field present on the interfaces (~1.5–4.5 V/Å), significant non-thermal coupling of rotational and translational motion of water molecules was clearly observed. Enhancement of the motion, manifested by increase of diffusivity, was detected in the first hydration layer, which is known to be heavily confined by adsorption to the TiO_2 surface. Interestingly, the diffusivity increases more rapidly on anatase than on rutile facets where the adsorbed water was found to be more organized and restrained. We observed that the applied oscillating field reduces number of hydrogen bonds on the interface. The remaining H-bonds are weaker than those detected under zero-field conditions; however, their lifetime increases on most of the surfaces when the low-frequency fields are applied. Reduction of adsorption interaction was observed also in IR spectra of interfacial water where the directional patterns are smeared as the intensities of applied fields increase. *Published by AIP Publishing.* [http://dx.doi.org/10.1063/1.4967520]

INTRODUCTION

Owing to its attractive properties, non-toxicity, and abundance in nature, titanium dioxide (titania, TiO_2) has been recognized by industry where it has been employed in many important applications such as hydrogen production, degradation of environmentally harmful organic compounds, or in paints.[1–5] From the three naturally occurring polymorphs of TiO_2—rutile, anatase, and brookite—it is anatase which is the most active and often found in nanomaterials, while rutile is the most thermodynamically stable.[6,7] From a technological perspective, rutile (110) and anatase (101) surface facets are the most important[8,9] and their properties and behavior have been extensively studied during recent decades. On the other hand, understanding of TiO_2/water interfaces, although crucial for fine-tuning of catalytic applications,[10] is still rather limited and research in this area is very active.

Accurate inelastic scattering experiments have shown that interfacial layer of water, adsorbed on a surface of titania, is heavily confined and its dynamical and vibrational features exhibit behavior more redolent of ice than liquid water.[11–14] This was later demonstrated computationally by classical molecular dynamics (MD) simulations.[15–22] Detail analyses of hydrogen bonding confirmed the layered structure of water on TiO_2 interface observed in experiments.[23–25] Structure of electric double layer (EDL) formed in an electrolyte in contact with the charged surface of titania was investigated by standing X-ray waves measurements[26] as well as by computer simulations.[27,28] Recently, a correlation between the depletion layer in TiO_2 subsurface and EDL was shown by Sang *et al.*[29] using classical MD.

Besides classical MD based on empirical potentials, density functional theory (DFT) proved to be very useful for investigating electro-chemical changes occurring on the TiO_2 surfaces.[30] Protonation and hydroxylation of titania in contact with water observed experimentally by STM,[31–34] potentiometric,[35] and spectroscopic measurements[36] were studied by many DFT studies which revealed important role of oxygen vacancies for catalytic activity.[37–40] While kinetics of these processes was recently measured by Petrik and Kimmel,[41] the influence of static electric field on oxygen vacancies at anatase (101) surface was studied by Selcuk and Selloni.[42] The extent of chemical adsorption of water on rutile (110) surface, which naturally depends on temperature and coverage, was extensively discussed in the recent literature.[43–45] Further, hydrogen bonds on the TiO_2/water interfaces have been studied by DFT-based MD,[46,47] which provided important insights into the vibrational modes of adsorbed water.

The effects of applied electric/electromagnetic field on TiO_2/water interfaces are of key interest for electrochemical applications of titania. The hydrogen-bonded water confined on TiO_2 surfaces might play an important role in stabilising solute by solvent interaction. On the other hand, it can hinder adsorption of molecules dissolved in an electrolyte that could be desired in catalysis. Therefore, the application of oscillating fields, which might potentially disrupt the interfacial hydrogen bonding and affect diffusivity, could possibly be employed to tune these properties. Recently, we investigated, using classical MD simulation techniques, how the first hydration layer of TiO_2 surfaces is influenced by external static electric fields.[48] We have shown that very strong intrinsic field of magnitude up

[a] Authors to whom correspondence should be addressed. Electronic addresses: zdenek.futera@ucd.ie, Fax: +353-1-7161177 and niall.english@ucd.ie, Tel.: +353-1-7161646, Fax: +353-1-7161177.

to 4.5 V/Å act on the adsorbed water, that the water is heavily confined, and that the external field does not lead to a considerable change in interfacial diffusivity. However, the response of hydrogen-bond lifetime and changes in librational as well as stretching band of IR spectra were also clearly observed. Here, we explore effects of oscillating electric fields of various intensities and frequencies, which were extensively studied on liquid bulk water by English *et al.*[49–56] We show that the applied oscillating fields affect the hydrogen bonding on the interface and leads to significant increases of diffusivity of the first hydration layer.

COMPUTATIONAL DETAILS

To investigate properties of water on various surfaces of titania, we built models of anatase (001), (101) and rutile (001), (100), (101), and (110) facets. The surface geometries were obtained by cutting bulk anatase ($I4_1/amd$ space group, tetragonal lattice, a = 3.785 Å, c = 9.514 Å) and rutile ($P4_2/mnm$ space group, tetragonal lattice, a = 4.593 Å, c = 2.959 Å).[57] Orthogonal supercells used in the simulations contained a surface slab comprising of 224 TiO_2 units and liquid part represented by 2000 water molecules of total density close to 1 g/cm^3. Cell dimensions and snapshots of the supercells are available in Ref. 48. The TiO_2 slab was described by empirical potential of Matsui and Akaogi[58] with parameters optimized by Bandura and Kubicki[59] and Predota *et al.*[15] The water molecules were described by the flexible Simple Point Charge (SPC) model.[60] To avoid numerical instabilities in the simulations we applied quartic potential $\frac{1}{2}k_2(r-r_0)^2 + \frac{1}{3}k_3(r-r_0)^3 + \frac{1}{4}k_4(r-r_0)^4$ form of H_w–O_w bond stretch rather than the Morse potential which we employed in the previous study.[48] The parameters k_2 = 1122.669 kcal/mol/Å^2, k_3 = −2822.096 kcal/mol/Å^2, k_4 = 1872.630 kcal/mol/Å^2, and r_0 = 1.0 Å were chosen to model the potential with the same location and curvature of the minimum as that of the previously used Morse curve (see Fig. S1, Supplementary Material). The potential was validated by calculating IR spectra of liquid water, which is shown in Fig. S2 of the Supplementary Material. As we are investigating non-dissociative structural and dynamical changes of interfacial hydration layers, the position of TiO_2 atoms was fixed in the simulations.

Typical structures of the interfaces are shown in Fig. 1 where different types of adsorbed water molecules are highlighted. Anatase (001) surface is flat with rows of 2-coordinated oxygen atoms (O_{2c}) exposed above the surface plane containing 5-coordinated titanium atoms (Ti_{5c}). The technologically more important anatase (101) has a terrace-like structure formed also by Ti_{5c} and O_{2c}, which is in contrast with anatase (001) located in different rows and therefore more accessible to contact with water. Flat surface of rutile (001) is characterized by presence of 4-coordinated Ti_{4c} interconnected with rows of O_{2c} which are arranged to form a corrugated, ridge-like structure. Rows of bridging oxygen atoms (O_b) attached to Ti_{5c} can be found on rutile (100) where the Ti_{5c}-O_b-Ti_{5c} planes are inclined as on anatase (101). This tilted pattern can be found also on the rutile (101) where the "chains" of O_{2c} are coordinated to surface Ti_{5c} atoms. Finally, surface plane formed by both Ti_{5c} and Ti_{6c} interconnected by O_{3c}, upon which characteristic rows of bridging O_b are exposed, is typical for the thermodynamically most stable rutile (110) facet. As indicated in Fig. 1, adsorbed water can be either coordinated to Ti_{5c} by O_w oxygen atoms or hydrogen-bonded to one or two O_{2c}/O_b by H_w hydrogen atoms, depending on the surface geometry.

Non-equilibrium MD simulations based on velocity Verlet algorithm[61] in the canonical (NVT) ensemble were performed by DL_POLY 4.07.[62] The equations of motion were propagated with a time step of 0.5 fs, while the temperature 300 K was imposed by a Nose-Hoover chain thermostat.[63,64] The thermostating was necessary to avoid heating of the system that would occur as a consequence of applied external oscillating electric field.[49] Long range electrostatic interactions were evaluated under periodic boundary conditions (PBCs) by the smooth particle-mesh Ewald (SPME) summation,[65] with a precision of 10^{-8}. The short-range van der Waals interactions were evaluated within a 10 Å cutoff. Forces acting

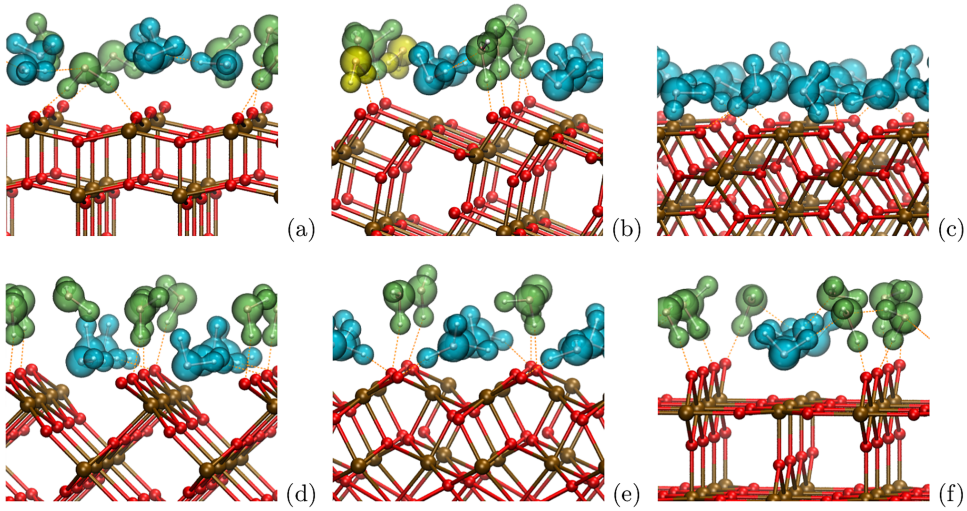

FIG. 1. Snapshots of TiO_2/water interfacial structures: (a) anatase (001), (b) anatase (101), (c) rutile (001), (d) rutile (100), (e) rutile (101), (f) rutile (110). Titanium atoms are shown in brown, with oxygen atoms in red. Only the first hydration layer is shown. Water molecules adsorbed to Ti_{5c}/Ti_{4c} by O_w are highlighted in cyan, molecules adsorbed to O_b/O_{2c} by one H_w in green, and those adsorbed to oxygen atoms by both H_w in yellow color.

on each charge site were affected by the oscillating electric field according to

$$m_i \ddot{\boldsymbol{r}}_i = \boldsymbol{f}_i + q_i E_{\max} \cos(\omega t)\, \boldsymbol{z}, \tag{1}$$

where q_i is the charge, $\boldsymbol{f}_i$ is the force on the site i, and $\boldsymbol{z}$ is unit vector oriented in z direction of laboratory coordinate system, which is perpendicular to the TiO_2 surface. Effects of the fields of RMS intensities E_{rms} = 0.05 V/Å, 0.10 V/Å, 0.15 V/Å, 0.20 V/Å, and 0.25 V/Å (noting that $E_{max} = \sqrt{2}E_{rms}$) and frequencies ν = 20.0 GHz, 25.0 GHz, 33.3 GHz, 50.0 GHz, and 100 GHz in the microwave region of the electromagnetic spectrum were explored. The field frequencies correspond to oscillating periods τ = 50 ps, 40 ps, 30 ps, 20 ps, and 10 ps, respectively. Although the applied intensities are higher than those routinely applied in electrochemistry, field strengths up to 0.5 V/Å may be obtained in experiments by applications of potentials of 1-5 kV onto tips of radius of 10-100 nm.[66] The production trajectories were 500 ps long, and therefore, at least 10 field cycles were carried out during each simulation, which was found sufficient for investigation of discussed properties. The applied field intensities are by one-order of magnitude lower than intrinsic electric fields found in bulk water[50,67] and on the TiO_2/water interfaces.[48] Note that the non-polarizable SPC water model cannot describe water polarization induced by the time-varying fields; however, it was shown by English *et al.*[49,50] that the influence of electromagnetic fields is described semi-quantitatively in this model comparing to polarizable potentials. The structural changes that could be induced by field intensities of 0.1 V/A and higher cannot be simulated using the SPC water model due to electrodissociation (dielectric breakdown). The results presented for this high-intensity range should be regarded as an extrapolation of the non-dissociative regime.

To analyze structural properties of adsorbed water, we calculated water O_w–H_w bond lengths, H_w–O_w–H_w valence angles, and individual-water dipoles as mean values $\langle x \rangle = \int x P(x) dx$ of corresponding normalized histograms $P(x)$ collected from the simulations. Similarly, histograms of hydrogen-bond lengths, angles, and average numbers of hydrogen bonds were computed. The hydrogen bonds were selected on the basis of geometry criteria for arrangement of donor (D), acceptor (A), and the hydrogen: the maximum allowed A-D distance was 3.5 Å and the A-D-H angle could not exceed 35°. Dynamics of the hydrogen bonds was described by Luzar-Chandler model[68] used for prediction of average hydrogen-bond lifetime. The self-diffusion constant of water was obtained using Einstein relation as a limit of mean-square displacement

$$D = \frac{1}{6} \lim_{t\to\infty} \frac{\langle (r(t_0+t) - r(t_0))\rangle}{t}. \tag{2}$$

Normalized autocorrelation functions (ACFs) $C(t) = \langle \boldsymbol{a_i}(t_0) \cdot \boldsymbol{a_i}(t_0+t)\rangle / \langle \boldsymbol{a_i}(t_0) \cdot \boldsymbol{a_i}(t_0)\rangle$ of internal water-molecule axes $\boldsymbol{a_1} = \boldsymbol{\mu}/|\boldsymbol{\mu}|$, $\boldsymbol{a_2} = \boldsymbol{h}/|\boldsymbol{h}|$, and $\boldsymbol{a_3} = \boldsymbol{a_1} \times \boldsymbol{a_2}$ (where $\boldsymbol{\mu}$ is a dipole-moment and h is H_w–H_w vector) were computed on the basis of Wiener-Khintchine relations employing fast Fourier transform (FFT) algorithm

$$\langle f(t_0) f(t_0+t)\rangle = \frac{1}{2\pi} \int \left| \int f(t') e^{-i\omega t'} dt' \right|^2 e^{i\omega t} d\omega. \tag{3}$$

Finally, the IR spectrum was computed as a power spectrum of the system-collective-dipole auto-correlation function,

$$I(\omega) \propto \omega^2 \int \langle \boldsymbol{M}(t_0) \boldsymbol{M}(t_0+t)\rangle e^{-i\omega t} dt, \tag{4}$$

where $\boldsymbol{M}(t)$ can be written as sum of individual water dipoles $\boldsymbol{M}(t) = \sum_i \boldsymbol{\mu}(t)$.

RESULTS AND DISCUSSION

First, we investigated structural properties of the interfacial layer. As we showed previously in Ref. 48 by calculating density profiles under zero-field conditions, water in the interface region exhibits characteristic layered structure given by interaction with surface. Typical orientations of adsorbed water molecules on the TiO_2 surfaces are shown in Fig. 1 where different types of interactions are distinguished by colors. The first-hydration-layer water can be coordinated to surface Ti_{4c}/Ti_{5c} atoms by O_w, which is a relatively strong interaction because the Ti_{4c}/Ti_{5c} atoms are unsaturated and positively charged. On the other hand, the water molecules can be hydrogen bonded to exposed surface O_{2c}/O_b atoms by H_w. This type of molecules can be found on all the studied surfaces except rutile (001) where each surface Ti_{4c} atom can coordinate two water molecules which leads to full coverage. However, even the Ti-adsorbed molecules can still be co-adsorbed by H-bonding to surface oxygen atoms on most of the surfaces enhancing their confinement. Finally, water molecules H-bonded to two neighboring O_b surface atoms by both their hydrogens H_w were found on anatase (101). These three types give rise to characteristic triple-peak structure of the first-hydration-layer density profile of anatase (101).[48]

While the position of the adsorbed water is found to be affected by application of static electric field on the system, where the H-bonded water molecules are pushed towards/outwards the surface depending on the orientation of the field with respect to the surface, no such effect was detected in oscillating field. Of course, the water molecules still respond to electric field by their dipole moments; however, the periodic nature of the field leads to averaging to zero-field position of the water layers when the system is detected for long enough time (that is much longer than period of one field cycle). In a similar way, we have not observed any changes in structural properties of individual water molecules. Their bond lengths (d_{OH}), valence angles (φ_{HOH}), and dipole moments (μ) were averaged to their zero-field values no matter what the intensity and frequency of external field was. Typical values obtained in the interface region near the TiO_2 surface are d_{OH} = 1.02–1.03 Å, φ_{HOH} = 102.9°–105.3°, and μ = 2.47–2.54 D comparing to the bulk region d_{OH} = 1.02 Å, φ_{HOH} = 105.4°, and μ = 2.44 D values.

Interestingly, the oscillating electric field has considerable effect on diffusivity in the interface region, which was not observed when the static fields were applied. On all studied TiO_2 surfaces, the diffusivity raises with increasing field intensity and frequency, although the effect is relatively minor on some of them. This is in agreement with behavior of bulk water where the large increase of mobility was detected earlier for non-polarizable water

model in frequency range up to 100 GHz[50]—the same increase of diffusivity was observed in the bulk region of the models studied in this work. The most substantial change was detected on anatase (001) where the zero-field diffusion constant $D = 7.59 \times 10^{-10}$ m^2/s grows to 2.21 $\times 10^{-9}$ m^2/s value, which is practically zero-field diffusion constant of bulk liquid water (2.8×10^{-9} m^2/s in our model), when the strong 0.25 V/Å of 100 GHz is applied on the system, as can be seen in Fig. 2. The increase is less pronounced at lower field frequencies, for example, $D = 1.29 \times 10^{-9}$ m^2/s was measured for the same field intensity but at the frequency 33.3 GHz. Similarly, diffusivity increased almost three-times on anatase (101) from zero-field 4.04×10^{-10} m^2/s to 1.14 $\times 10^{-9}$ m^2/s. The field effect on rutile facets is a bit smaller (increase by 170%–240% relative to the zero-field) though still clearly observable on all studied surfaces. Specifically, the diffusion constant of 3.70×10^{-10} m^2/s rises to 7.71 $\times 10^{-10}$ m^2/s when field of 0.25 V/Å intensity and frequency 100 GHz is applied on rutile (110).

To analyze the observed differences in diffusivities on the various TiO_2 surfaces, we evaluated auto-correlation functions (ACFs) of water-molecule internal axes. We defined the axes as $\boldsymbol{a_1} = \boldsymbol{\mu}/|\boldsymbol{\mu}|$, $\boldsymbol{a_2} = \boldsymbol{h}/|\boldsymbol{h}|$, and $\boldsymbol{a_3} = \boldsymbol{a_1} \times \boldsymbol{a_2}$, where $\boldsymbol{\mu}$ and $\boldsymbol{h}$ are dipole-moment and H_w–H_w vectors, respectively. Since the water molecules interact with the external field via their dipole moments, rotation of the molecules as a response to the field can be expected, as was observed in liquid water.[54] Indeed, this behavior is manifested by visible oscillations in ACF of $\boldsymbol{a}_1$ shown in Fig. 3. Interestingly, only on anatase (001) does the ACF decay to the limiting value of zero regardless of applied-field intensity and frequency as is typical for liquid water (cf. Fig. S3a, Supplementary Material). Water adsorbed on this surface is not so heavily confined like on the other facets.

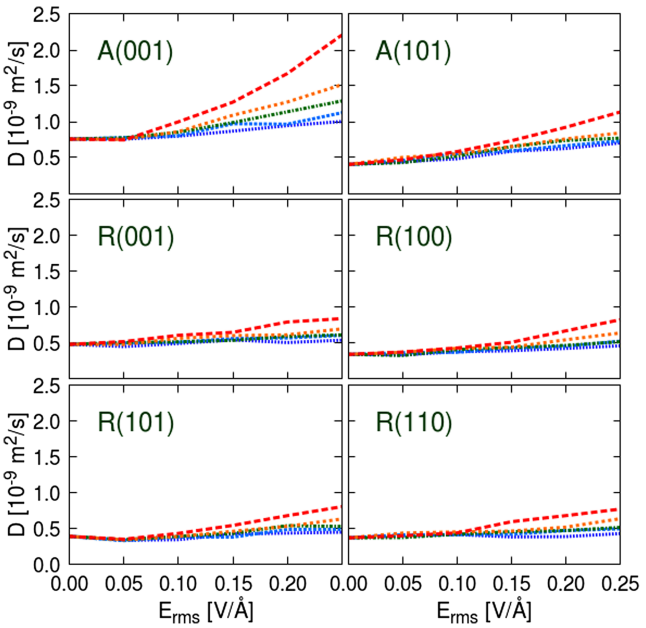

FIG. 2. Water self-diffusion coefficient D calculated for the first hydration layer of TiO_2 surfaces. The oscillating field of frequencies 20 GHz (dark blue), 25 GHz (light blue), 33 GHz (green), 50 GHz (orange), and 100 GHz (red) was applied on the system. The zero-field diffusion constant in bulk water region was found to be 2.8×10^{-9} m^2/s.

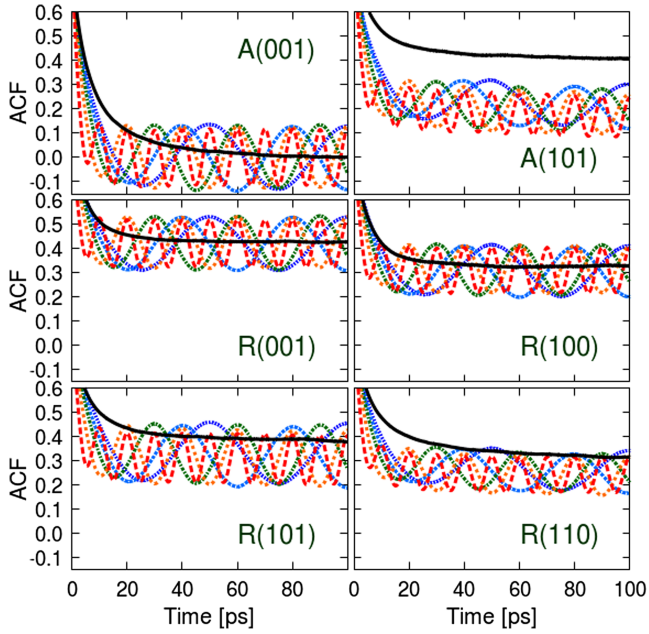

FIG. 3. Autocorrelation function (ACF) of the water-molecule dipole direction calculated for the first hydration layer of TiO_2 surfaces. The oscillating field of intensity 0.25 V/Å and frequencies 20 GHz (dark blue), 25 GHz (light blue), 33 GHz (green), 50 GHz (orange), and 100 GHz (red) were applied on the system. ACF calculated under zero-field conditions is shown in solid black line for comparison.

The reason lies in the configuration of the Ti5c surface atoms which are located on the same row as the exposed O_{2c} atoms and therefore they are less accessible for water. Accordingly, weaker adsorption interactions can be expected there which results in the extraordinary increase of the diffusivity with applied oscillating field discussed above. Completely opposite situation can be seen on rutile (001). Water on this surface is strongly adsorbed to Ti_{5c} by O_w and the confinement is intensified by hydrogen bonding to neighboring O_{2c} atoms. This fixation is manifested by the relatively high correlation of dipoles which simply "sway" near their zero-field positions as the oscillating field is applied and they scarcely leave the adsorption site. Therefore the rise of diffusivity is minimal on this surface.

Similar to rutile (001), the (100) surface of this polymorph exhibits rather strong water confinement because of the suitable surface geometry allowing simultaneous adsorption of water to Ti_{5c} atoms and H-bonding to bridging oxygen atoms O_b. However, small decrease of corresponding ACF mean value can be seen in Fig. 3 indicating that the applied fields help, at least partly, to release the water from their constrained positions and thus increase the diffusivity. This effect is even larger on the rutile (101) and (110) surfaces where the reduced correlation is clearly visible. The greatest change of ACF was detected on anatase (101) where the correlation is reduced by 50% when the strong fields of 0.25 V/Å intensity are applied. The effects of the weaker fields are qualitatively the same as those discussed here; however, oscillation magnitudes of ACF and changes in their mean values with respect to zero-field conditions are smaller. No visible effects of the external field on the system dynamics were observed for intensities smaller than 0.05 V/Å. This threshold RMS electric field intensity has

been also determined for pure bulk water in previous works of English *et al.*[50]

Further, we investigated rotation of water molecules around their main axis (dipole-moment direction, $\boldsymbol{a}_1$) by calculating the auto-correlation functions of the $\boldsymbol{a}_2$ axis (H–H direction, shown in Fig. 4) and the $\boldsymbol{a}_3$ axis (perpendicular to $\boldsymbol{a}_1$ and $\boldsymbol{a}_2$, plotted in Fig. S4 of the Supplementary Material). These two ACFs look rather similar when they are calculated for liquid water under the influence of oscillating electric fields (compare Figs. S3b and S3c of the Supplementary Material). They decrease to zero quickly during first ~20 ps in case of $\boldsymbol{a}_2$ and even more rapidly in case of $\boldsymbol{a}_3$ (~15 ps). Increasing intensities and frequencies of the applied fields lead to shorter correlations times, which was detected also for liquid water by Reale *et al.*[55] This behavior was also observed in hydration layers of anatase (001), rutile (001), and rutile (100) surfaces, although the decay time (~40 ps) under zero-field conditions is longer than in liquid water case because the water orientation is confined by adsorption. Much longer correlation time exhibits rutile (110) and especially rutile (101) interfaces where the rotations are apparently more hindered. Finally, anatase (101) surface is rather atypical, exhibiting large correlation of rotational movements under zero-field conditions; however, these are rapidly reduced when the oscillating field is applied on the system. It suggests that the well-organized layered structure of this interface, maintained by hydrogen bonding of water to the surface as well as lateral H-bonding within the hydration layer, is considerably affected by the oscillating fields which promote the water rotations.

The hydrogen bonds are characterized by their bond lengths, angles, and lifetimes. We evaluated these quantities for the H-bonds between water H_w atoms and surface O_{2c}/O_b atoms to elucidate changes in adsorption of the first hydration layer. Field effects on the bond lengths, which can be directly correlated with H-bond strengths, are plotted in Fig. S5 (Supplementary Material) while the effects on the H-bond angles are shown in Fig. S6 of the Supplementary Material. The shortest, and therefore strongest, H-bonds can be found on rutile (101) with lengths ~1.56 Å, while the weakest interaction is on anatase (001) surface where the bonds are ~1.80 Å long (compare with 1.95 Å calculated for the bulk water). Considerable field effects were detected practically only on anatase (101) where the lengths of H-bonds increase from zero-field value of 1.66 to 1.78 Å when 100 GHz field of 0.25 V/Å intensity is applied to the interface. This is in accordance with enhanced rotations and larger diffusivity observed on the (101) surface. It also correlates with average number of hydrogen bonds per water molecule that is reduced from 2.72 to 1.82 on this interface (see Fig. S7 of the Supplementary Material for details).

Next, we investigated dynamical behavior of the hydrogen bonds by calculating their average lifetime using the Luzar-Chandler model.[68] As we already observed when we studied effect of static electric fields, the response of the H-bond lifetimes is somewhat unique for each of the explored TiO_2 surfaces. Effects of the oscillating fields are shown in Fig. 5, noting that the average lifetime of 2.64 ps was obtained for liquid bulk water under zero-field conditions. In general, the interface hydrogen-bond lifetime increases with the applied fields on all the interfaces except anatase (001) where a decrease was observed. Low-frequency fields with long oscillating periods (20 GHz–50 ps) lead to longer lifetimes than those observed at high-frequencies as the water molecule movement is relatively slow and the hydrogen bonds kinetics of breakage and reformation is not accelerated by faster field rotations.

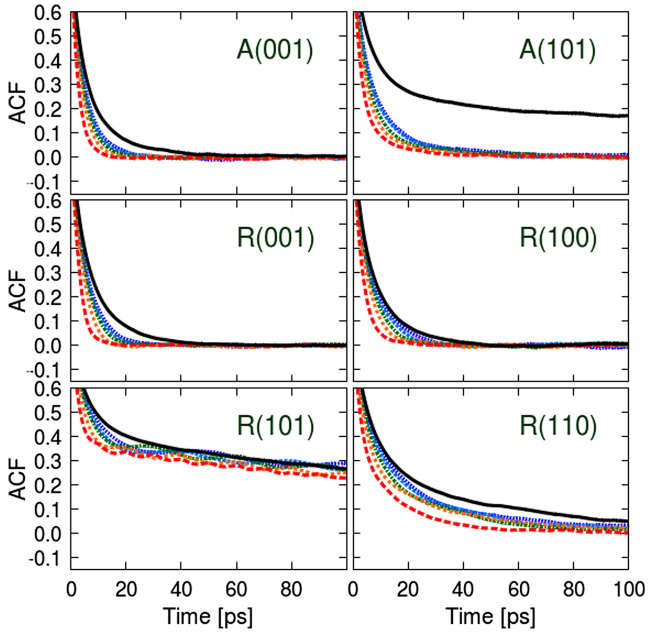

FIG. 4. Autocorrelation function (ACF) of water-molecule H–H direction calculated for the first hydration layer of TiO_2 surfaces. The oscillating field of intensity 0.25 V/Å and frequencies 20 GHz (dark blue), 25 GHz (light blue), 33 GHz (green), 50 GHz (orange), and 100 GHz (red) were applied on the system. ACF calculated under zero-field conditions is shown in solid black line for comparison.

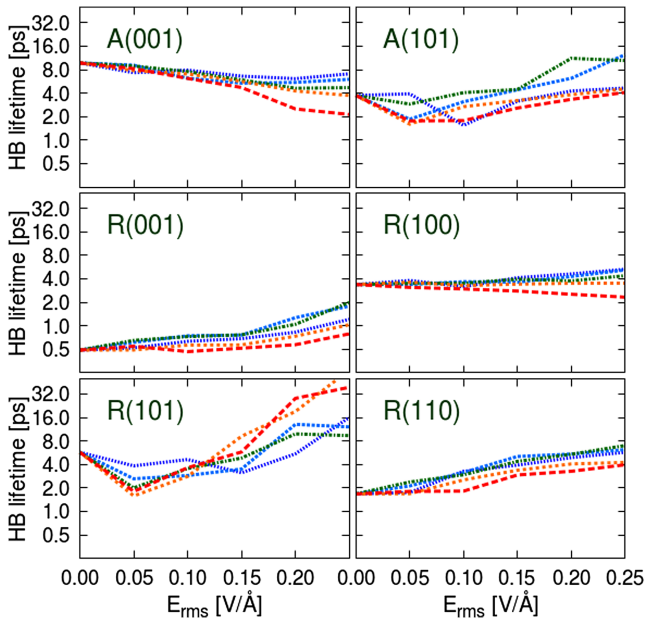

FIG. 5. Average hydrogen-bond (HB) lifetime calculated for the first hydration layer of TiO_2 surfaces. The oscillating field of frequencies 20 GHz (dark blue), 25 GHz (light blue), 33 GHz (green), 50 GHz (orange), and 100 GHz (red) was applied on the system. The lifetime was obtained from the Luzar-Chandler model of HB kinetics.

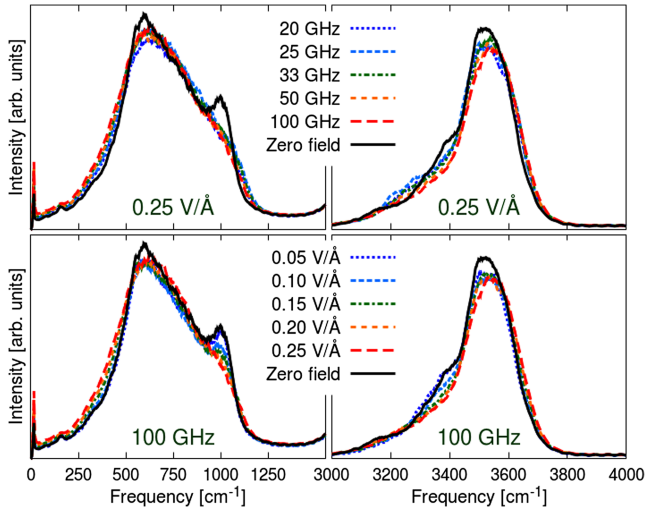

FIG. 6. Effect of oscillating electric fields on libration band (left-side panels) and vibration band (right-side panels) of IR spectra calculated on anatase (101) interface.

Finally, we show field effects on the librational and vibrational bands of IR spectra calculated for interfacial water region on anatase (101) surface (Fig. 6) and rutile (110) surface (Fig. 7). In the anatase case, only minor changes can be observed on the main librational peak at 530 cm^{-1}, which is in accordance with bulk water behavior.[55] The latter peak near 1000 cm^{-1} originates from water movement along the surface ridges on that anatase (101) surface, as we have shown in Ref. 48, and this directional preference is clearly decreasing as the external-field intensity increases. As for the vibrational band, the peak located around 3500 cm^{-1} is slightly blue-shifted although any more significant changes are not visible. Similar changes are observable on rutile (110) interface. As in the anatase case, the directional preference in the librational band, where the 1000 cm^{-1} peak indicates movement along the surface O_b chains, becomes less important as the field intensities increase. Similar trend can be seen on 3150 cm^{-1} peak in the vibrational band, which stems exclusively from stretches

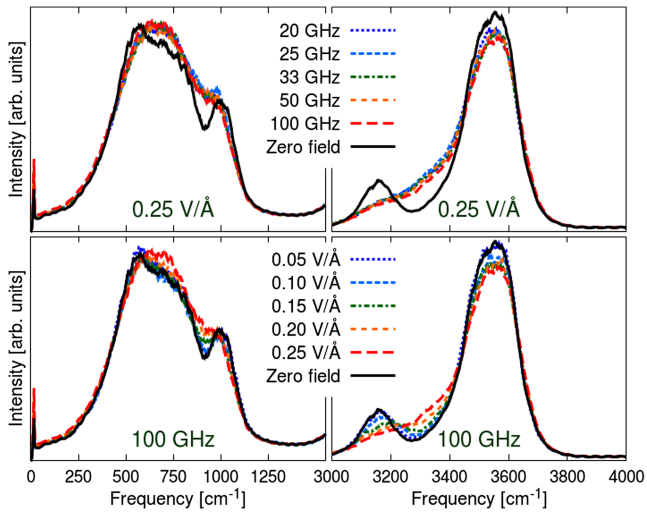

FIG. 7. Effect of oscillating electric fields on libration band (left-side panels) and vibration band (right-side panels) of IR spectra calculated on rutile (110) interface.

in z direction perpendicular to the surface. The observed oscillating field effects on the IR spectra are qualitatively similar to the effects of static field applied in the surface-parallel direction, which was shown to decrease adsorption interaction of the first hydration layer.[48] We can therefore conclude that the application of oscillating electric fields on the TiO_2/water interfaces reduces the adsorption by disrupting hydrogen-bond network, as a result of torques acting on the water molecules, and it thus lowers the water confinement and increases its mobility.

CONCLUSIONS

We have carried out non-equilibrium MD simulations of TiO_2 anatase (001), (101) and rutile (001), (100), (101), and (110) interfaces influenced by external oscillating electric fields of intensities 0.05 V/Å, 0.10 V/Å, 0.15 V/Å, 0.20 V/Å, and 0.25 V/Å and frequencies 20.0 GHz, 25.0 GHz, 33.3 GHz, 50.0 GHz, and 100 GHz. We have found out that in contrast to static electric field, the external oscillating fields considerably affect diffusivity in the interface region. The diffusivity raised by 280%–290% from the zero-field value on anatase facets and by 170%–240% on the rutile surfaces. By analyzing the auto-correlation functions of internal water-molecule axes, we demonstrated that the hydration layer is more confined and organized on the rutile interfaces than on the anatase ones. The correlation of water dipole-direction is high under zero-field conditions and only partly reduced when the oscillating field is applied on rutile structures. This contrasts with anatase surfaces, where the water molecules are practically freely rotating on the (001) facet even under zero-free conditions, whilst the regular structure arrangement is rather easily disrupted by applied field on the (101) surface.

Analyses of hydrogen bonding between the first hydration layer and TiO_2 surfaces have indicated that, as the applied fields interact with the water-molecule dipole moments and induce their movements, the average number of H-bond per molecule decreases. The remaining bonds are longer, and therefore weaker, on anatase (101) and rutile (110) compared to their zero-field lengths. The kinetics of the hydrogen bonds was found rather complex, and affected not only by applied field, but also by molecular arrangement on each surface. In general, the hydrogen-bond lifetime gets longer with increasing intensity of the field—except for anatase (001) where the opposite trend was observed. However, higher frequencies inducing more rapid rotations of water molecules in the interface region have tendency to lower the H-bond lifetime. The rotational movement of adsorbed water also smears the directional patterns in IR spectra calculated on TiO_2 interfaces. The oscillating electric field therefore reduces the TiO_2/water interaction and thus increases the water mobility on the interface.

SUPPLEMENTARY MATERIAL

See Supplementary Material for profile of H_w–H_w stretching potential, IR spectrum of bulk water, autocorrelation function of internal water-molecule axes in bulk water,

autocorrelation function of water-molecule axis perpendicular to its dipole moment and H–H direction for hydration layers, mean values of hydrogen bond lengths, angles, and number as function of external field intensity and frequency.

ACKNOWLEDGMENTS

The authors thank Science Foundation Ireland for funding under Grant No. SFI 15/ERC-I3142.

[1] A. Fujishima and K. Honda, "Electrochemical photolysis of water at a semiconductor electrode," Nature **238**, 37–38 (1972).
[2] U. Diebold, "The surface science of titanium dioxide," Surf. Sci. Rep. **48**, 53–229 (2003).
[3] M. A. A. Henderson, "Surface science perspective on TiO_2 photocatalysis," Surf. Sci. Rep. **66**, 185–297 (2011).
[4] K. Bourikas, C. Kordulis, and A. Lycourghiotis, "Titanium dioxide (anatase and rutile): Surface chemistry, liquid-solid interface chemistry, and scientific synthesis of supported catalyst," Chem. Rev. **114**, 9754–9823 (2014).
[5] B. O'Regan and M. Gratzel, "A low-cost, high-efficiency solar cell based on dye-sensitized colloidal TiO_2 films," Nature **353**, 737–740 (1991).
[6] H. Zhang and J. F. Banfield, "Thermodynamical analysis of phase stability of nanocrystalline titania," J. Mater. Chem. **8**(9), 2073–2076 (1998).
[7] M. R. Ranade, A. Navrotsky, H. Z. Zhang, J. F. Banfield, S. H. Elder, A. Zaban, P. H. Borse, S. K. Kulkarni, G. S. Doran, and H. J. Whitfield, "Energetics of nanocrystalline TiO_2," Proc. Natl. Acad. Sci. U. S. A. **99**, 6476–6481 (2002).
[8] N.-G. Park, J. van de Lagemaat, and A. J. Frank, "Comparison of dye-sensitized rutile- and anatase-based TiO_2 solar cells," J. Phys. Chem. B **104**, 8989–8994 (2000).
[9] C. L. Pang, R. Lindsay, and G. Thornton, "Structure of clean and adsorbate-covered single-crystal rutile TiO_2 surfaces," Chem. Rev. **113**, 3887–3948 (2013).
[10] C. L. Pang, R. Lindsay, and G. Thornton, "Chemical reactions on rutile TiO_2(110)," Chem. Soc. Rev. **37**, 2328–2353 (2008).
[11] A. A. Levchenko, A. I. Kolesnikov, N. L. Ross, B. F. Woodfield, G. Li, A. Navrotsky, and J. Boerio-Goates, "Dynamics of water confined on a TiO_2 (anatase) surface," J. Phys. Chem. A **111**(49), 12584–12588 (2007).
[12] E. R. Spencer, A. A. Levchenko, N. L. Ross, A. I. Kolesnikov, J. Boerio-Goates, B. F. Woodfield, A. Navrotsky, and G. Li, "Inelastic neutron scattering study of confined surface water on rutile nanoparticles," J. Phys. Chem. A **113**(12), 2796–2800 (2009).
[13] E. Mamontov, D. J. Wesolowski, L. Vlcek, P. T. Cummings, J. Rosenqvist, W. Wang, and D. R. Cole, "Dynamics of hydration water on rutile studied by backscattering neutron spectroscopy and molecular dynamics simulation," J. Phys. Chem. C **112**, 12334–12341 (2008).
[14] E. Mamontov, L. Vlcek, D. J. Wesolowski, P. T. Cummings, J. Rosenqvist, W. Wang, D. R. Cole, L. M. Anovitz, and G. Gasparovic, "Suppression of the dynamic transition in surface water at low hydration levels," Phys. Rev. E **79**, 051504 (2009).
[15] M. Predota, A. V. Bandura, P. T. Cummings, J. D. Kubicki, D. J. Wesolowski, A. A. Chialvo, and M. L. Machesky, "Electric double layer at the rutile (110) surface. 1. Structure of surfaces and interfacial water from molecular dynamics by use of *ab initio* potentials," J. Phys. Chem. B **108**, 12049–12060 (2004).
[16] Z. Zhao, Z. Li, and Z. Zou, "Structure and properties of water on the anatase TiO_2(101) surface: From single-molecule adsorption to interface formation," J. Phys. Chem. C **116**, 11054–11061 (2012).
[17] H. Nakamura, T. Ohto, and Y. Nagata, "Polarizable site charge model at liquid/solid interfaces for describing surface polarity: Application to structure and molecular dynamics of water/rutile TiO_2(110) interface," J. Chem. Theory Comput. **9**, 1193–1201 (2013).
[18] R. S. Kavathekar, P. Dev, N. J. English, and J. M. D. MacElroy, "Molecular dynamics study of water in contact with the TiO_2 rutile-110 100, 101, 001 and anatase-101, 001 surface," Mol. Phys. **109**(13), 1649–1656 (2011).
[19] R. S. Kavathekar, N. J. English, and J. M. D. MacElroy, "Study of translational, librational and intra-molecular motion of adsorbed liquid monolayers at various TiO_2 interfaces," Mol. Phys. **109**(22), 2645–2654 (2011).
[20] R. S. Kavathekar, N. J. English, and J. M. D. MacElroy, "Spatial distribution of adsorbed water layers at the TiO_2 rutile and anatase interfaces," Chem. Phys. Lett. **554**, 102–106 (2012).
[21] N. J. English, "Dynamical properties of physically adsorbed water molecules at the TiO_2 rutile-(110) surface," Chem. Phys. Lett. **583**, 125–130 (2013).
[22] N. J. English, "Diffusivity and mobility of adsorbed water layers at TiO_2 rutile and anatase interfaces," Crystals **6**, 1 (2016).
[23] N. J. English, R. S. Kavathekar, and J. M. D. MacElroy, "Hydrogen bond dynamical properties of absorbed liquid water monolayers with various TiO_2 interfaces," Mol. Phys. **110**(23), 2919–2925 (2012).
[24] T. Ohto, A. Mishra, S. Yoshimune, H. Nakamura, M. Bonn, and Y. Nagata, "Influence of surface polarity on water dynamics at the water/rutile TiO_2(110) interface," J. Phys. Condens. Matter **26**, 244102 (2014).
[25] A. Y. Nosaka, T. Fujiwara, H. Yagi, H. Akutsu, and Y. Nosaka, "Characteristics of water adsorbed on TiO_2 photocatalytic systems with increasing temperature as studied by solid-state ^{1}H NMR spectroscopy," J. Phys. Chem. B **108**, 9121–9125 (2004).
[26] P. Fenter, L. Cheng, S. Rihs, M. Machesky, M. J. Bedzyk, and N. C. Sturchio, "Electrical double-layer structure at the rutile-water interface as observed *in situ* with small-period X-ray standing waves," J. Colloid Interface Sci. **225**, 154–165 (2000).
[27] M. Predota, P. T. Cummings, Z. Zhang, P. Fenter, and D. J. Wesolowski, "Electric double layer at the rutile (110) surface. 2. Adsorption of ions from molecular dynamics and X-ray experiments," J. Phys. Chem. B **108**, 12061–12072 (2004).
[28] M. Predota, P. T. Cummings, and D. J. Wesolowski, "Electric double layer at the rutile (110) surface. 3. Inhomogeneous viscosity and diffusivity measurement by computer simulations," J. Phys. Chem. C **111**, 3071–3079 (2007).
[29] L. Sang, Y. Zhang, J. Wang, Y. Zhao, and Y. Chen, "Correlation of the depletion layer with the helmholtz layer in the anatase TiO_2-H_2O interface via molecular dynamics simulations," Phys. Chem. Chem. Phys. **18**, 15427–15435 (2016).
[30] F. De Angelis, C. Di Valentin, S. Fantacci, A. Vittadini, and A. Selloni, "Theoretical studies of anatase and less common TiO_2 phases: Bulk, surfaces, and nanomaterials," Chem. Rev. **114**, 9708–9753 (2014).
[31] S. Wendt, R. Schaub, J. Matthiesen, E. K. Vestergaard, E. Wahlstrom, M. D. Rasmussen, P. Thostrup, L. M. Molina, E. Laegsgaard, I. Stensgaard, B. Hammer, and F. Besenbacher, "Oxygen vacancies on TiO_2(110) and their interaction with H_2O and O_2: A combined high-resolution STM and DFT study," Surf. Sci. **598**, 226–245 (2005).
[32] Y. He, A. Tilocca, O. Dulub, A. Selloni, and U. Diebold, "Local ordering and electronic signatures of submonolayer water on anatase TiO_2(101)," Nat. Mater. **8**, 585–589 (2009).
[33] Z.-T. Wang, J. C. Garcia, N. A. Deskins, and I. Lyubinetsky, "Ability of TiO_2(110) surface to be fully hydroxylated and fully reduced," Phys. Rev. B **92**, 081402 (2015).
[34] J. Lee, D. C. Sorescu, X. Deng, and K. D. Jordan, "Water chain formation on TiO_2 (110)," J. Phys. Chem. Lett. **4**, 53–57 (2013).
[35] M. K. Ridley, M. L. Machesky, D. A. Palmer, and D. J. Wesolowski, "Potentiometric studies of the rutile–water interface: Hydrogen-electrode concentration-cell versus glass-electrode titrations," Colloids Surf., A **204**, 295–308 (2002).
[36] H. P. Marques, A. R. Canario, A. M. C. Moutinho, and O. M. N. D. Teodoro, "Tracking hydroxyl adsorption on TiO_2(110) through secondary emission changes," Appl. Surf. Sci. **255**, 7389–7393 (2009).
[37] U. Aschauer, Y. He, H. Cheng, S.-C. Li, U. Diebold, and A. Selloni, "Influence of subsurface defects on the surface reactivity of TiO_2: Water on anatase (101)," J. Phys. Chem. C **114**, 1278–1284 (2010).
[38] H. Cheng and A. Selloni, "Hydroxide ions at the water/anatase TiO_2(101) interface: Structure and electronic states from first principles molecular dynamics," Langmuir **26**(13), 11518–11525 (2010).
[39] A. Tilocca and A. Selloni, "DFT-GGA and DFT+U simulations of thin water layers on reduced TiO_2 anatase," J. Phys. Chem. C **116**, 9114–9121 (2012).
[40] L.-M. Liu, P. Crawford, and P. Hu, "The interaction between adsorbed OH and O_2 on TiO_2 surfaces," Prog. Surf. Sci. **84**, 155–176 (2009).
[41] N. G. Petrik and G. A. Kimmel, "Reaction kinetics of water molecules with oxygen vacancies on rutile TiO_2(110)," J. Phys. Chem. C **119**, 23059–23067 (2015).
[42] S. Selcuk and A. Selloni, "Influence of external electric fields on oxygen vacancies at the anatase (101)," Surf. J. Chem. Phys. **141**, 084705 (2014).
[43] C. Z. Liu, G. Thornton, A. Michaelides, and C. Zhang, "Structure and dynamics of liquid water on rutile TiO_2(110)," Phys. Rev. B **82**, 161415 (2010).
[44] D. J. Wesolowski, J. O. Sofo, A. V. Bandura, Z. Zhang, E. Mamontov, M. Predota, N. Kumar, J. D. Kubicki, P. R. C. Kent, L. Vlcek *et al.*,

"Comment on 'Structure and dynamics of liquid water on rutile TiO_2 (110)'," Phys. Rev. B **85**, 167401 (2012).
[45]M. L. Liu, C. Zhang, G. Thornton, and A. Michaelides, "Reply to 'Comment on "Structure and dynamics of liquid water on rutile TiO_2 (110)"'," Phys. Rev. B **85**, 167402 (2012).
[46]G. Mattioli, F. Filippone, R. Caminiti, and A. A. Bonapasta, "Short hydrogen bonds at the water/TiO_2 (anatase) interface," J. Phys. Chem. C **112**, 13579–13586 (2008).
[47]N. Kumar, S. Neogi, P. R. C. Kent, A. V. Bandura, J. D. Kubicki, D. J. Wesolowski, D. Cole, and J. O. Sofo, "Hydrogen bonds and vibrations of water on (110) rutile," J. Phys. Chem. C **113**, 13732–13740 (2009).
[48]Z. Futera and N. J. English, "Electric-field effects on adsorbed-water structural and dynamical properties at rutile and anatase-TiO_2 surfaces," J. Phys. Chem. C **120**(35), 19603–19612 (2016).
[49]N. J. English and J. M. D. MacElroy, "Molecular dynamics simulations of microwave heating of water," J. Chem. Phys. **118**, 1589–1592 (2003).
[50]N. J. English and J. M. D. MacElroy, "Hydrogen bonding and molecular mobility in liquid water in external electromagnetic fields," J. Chem. Phys. **119**, 11806–11813 (2003).
[51]N. J. English, "Molecular dynamics simulations of microwave effects on water using different long-range electrostatic methodologies," Mol. Phys. **104**, 243–253 (2006).
[52]N. J. English and C. J. Waldron, "Perspectives on external electric fields in molecular simulation: Progress, prospects and challenges," Phys. Chem. Chem. Phys. **77**, 12407–12440 (2015).
[53]N. J. English, P. G. Kusalik, and S. A. Woods, "Coupling of translational and rotational motion in chiral liquids in electromagnetic and circularly polarized electric fields," J. Chem. Phys. **136**, 094508 (2012).
[54]R. Reale, N. J. English, P. Marracino, M. Liberti, and F. Apollonio, "Dipolar response and hydrogen-bond kinetics in liquid water in square-wave time-varying electric fields," Mol. Phys. **112**, 1870 (2013).
[55]R. Reale, N. J. English, P. Marracino, M. Liberti, and F. Apollonio, "Translational and rotational diffusive motion in liquid water in square-wave time-varying electric fields," Chem. Phys. Lett. **582**, 60 (2013).
[56]M. Avena, P. Marracino, M. Liberti, F. Apollonio, and N. J. English, "Communication: Influence of nanosecond-pulsed electric fields on water and its subsequent relaxation: Dipolar effects and debunking memory," J. Chem. Phys. **142**, 141101 (2015).
[57]D. T. Cromer and K. Herrington, "The structures of anatase and rutile," J. Am. Chem. Soc. **77**, 4708–4709 (1955).
[58]M. Matsui and M. Akaogi, "Molecular dynamics simulations of the structural and physical properties of the four polymorphs of TiO_2," Mol. Simul. **6**, 239–244 (1991).
[59]A. V. Bandura and J. D. Kubicki, "Derivation of force field parameters for TiO_2-H_2O systems from *ab initio* calculations," J. Phys. Chem. B **107**(40), 11072–11081 (2003).
[60]K. Toukan and A. Rahman, "Molecular-dynamics study of atomic motions in water," Phys. Rev. B **31**(5), 2643–2648 (1985).
[61]W. C. Swope, C. Andersen, P. H. Berens, and K. R. Wilson, "A computer simulation method for the calculation of equilibrium constants for the formation of physical clusters of molecules: Application to small water clusters," J. Chem. Phys. **76**, 637–649 (1982).
[62]I. T. Todorov, W. Smith, K. Trachenko, and M. T. Dove, "DL_POLY_3: New dimension in molecular dynamics simulations via massive parallelism," J. Mater. Chem. **16**, 1911–1918 (2006).
[63]S. Nose, "A unified formulation of the constant temperature molecular dynamics methods," J. Chem. Phys. **81**, 511–519 (1984).
[64]W. G. Hoover, "Canonical dynamics: Equilibrium phase-space distributions," Phys. Rev. A **31**, 1695–1697 (1985).
[65]U. Essmann, L. Perera, M. L. Berkowitz, T. Darden, H. Lee, and L. G. Pedersen, "A smooth particle mesh Ewald method," J. Chem. Phys. **103**, 8577–8593 (1995).
[66]D. L. Scovell, T. D. Pinkerton, V. K. Medvedev, and E. M. Stuve, "Phase transitions in vapor-depositied water under the influence of high surface electric fields," Surf. Sci. **457**, 365–376 (2000).
[67]B. Sellner, M. Valiev, and S. M. Kathmann, "Charge and electric field fluctuations in aqueous NaCl electrolytes," J. Phys. Chem. B **117**(37), 10869–10882 (2013).
[68]A. Luzar and D. Chandler, "Hydrogen-bond kinetics in liquid water," Nature **379**, 55–57 (1996).